



36 **Abstract**

37 The organizational role for hormones in the regulation of sexual behavior is currently poorly  
38 explored. Previous work showed that seasonal variation in levels of the steroid hormone 20-  
39 hydroxyecdysone (20E) during pupal development regulates plasticity in male courtship behavior  
40 in *Bicyclus anynana* butterflies. Wet season (WS) males, reared at high temperature, have high  
41 levels of 20-hydroxyecdysone (20E) during pupation and become active courters. Dry season  
42 (DS) males, reared at low temperatures, have lower levels of 20E and lower courtship rates.  
43 Rescue of WS courtship rates can be achieved via injection of 20E into DS male pupae, but it is  
44 still unknown whether 20E alters gene expression in the pupal brain, and if so, the identity of  
45 those targets. Using transcriptomics, qPCR, and behavioral assays with a transgenic knockout, we  
46 show that higher expression levels of the *yellow* gene in DS male pupal brains, relative to WS  
47 brains, represses courtship in DS males. Furthermore, injecting DS males with 20E downregulates  
48 *yellow* to WS levels 4 hours post-injection, revealing a hormone sensitive window that determines  
49 courtship behavior. These findings are in striking contrast to *Drosophila*, where *yellow* is required  
50 for active male courtship behavior. We conclude that 20E plays an organizational role during  
51 pupal brain development by regulating the expression of *yellow*, which is a repressor of the neural  
52 circuitry for male courtship behavior in *B. anynana*. This work shows that similar to vertebrates,  
53 hormones can also play an organizational role in insect brains, leading to permanent changes in  
54 adult sexual behavior.

55

56

57 **Significance Statement**

58 Behavioral plasticity in adult insects is known to be regulated by hormones, which activate  
59 neural circuits in response to environmental cues. Here, we show that hormones can also regulate  
60 adult behavioral plasticity by altering gene expression during brain development, adjusting the  
61 insect's behavior to predictable seasonal environmental variation. We show that seasonal  
62 changes in the hormone 20E alters expression of the *yellow* gene in the developing pupal brain of  
63 *Bicyclus anynana* butterflies, which leads to differences in male courtship behavior between the  
64 dry and wet seasonal forms. This work provides one of the first examples of the organizational  
65 role of hormones in altering gene expression and adult sexual behavior in the developing insect  
66 brain.

67

## 68 **Introduction**

69 Behavioral plasticity is essential for animals to adapt to environmental variation and it is often  
70 triggered by hormonal changes that organize or activate neural circuits in the brain (1-3).  
71 Seasonal changes in temperature and photoperiod can serve as important cues that alter hormone  
72 levels and sexual behavior in a wide range of vertebrate and invertebrate taxa (4). Precisely how  
73 hormone signaling influences sexual behavior in most animals however, is not well known (5).  
74 In vertebrates, hormones are considered to play both a brain organizational role, during  
75 development, as well as a behavioral activational role in adults, compared to just an adult  
76 activational role in insects (6, 7). This conceptual framework describes whether hormones  
77 permanently organize neural circuitry during early critical periods that later influence adult  
78 behavior, or whether they modulate behavior by activating existing neural circuits in response to  
79 external cues (7, 8).

80  
81 Sexual behavior in insects has traditionally been viewed as a consequence of cell-autonomous  
82 processes taking place during brain development, and involving sex determination genes (6) such  
83 as *fruitless* and *doublesex* (9). The role of insect hormones is typically described as playing an  
84 activational role, allowing rapid and reversible behavioral changes, such as activating neural  
85 circuits that regulate pheromone communication or sexual receptivity (10-13). However,  
86 hormones have also been proposed to play an organizational role in insects, for instance in the  
87 regulation of behavioral polyphenisms in honeybees and locusts (7) and sexual maturity in  
88 *Drosophila* (14). Yet, no evidence is available for the organizational role of steroid hormones in  
89 driving sexual behaviors in adult insects, similar to the role of steroid hormones in vertebrate  
90 sexual differentiation, where exposure to different hormone levels during ontogeny leads to  
91 discrete, fixed differences in neural development and sexual behaviors (7).

92  
93 For insects living in seasonal environments, hormones could play an organizational role earlier in  
94 development to ensure that sexual behavior is optimized for particular environmental conditions  
95 that will be prevalent upon adult emergence (15). An example of a species where such a brain  
96 organizational role may be happening is the African seasonal polyphenic butterfly, *Bicyclus*  
97 *anynana*. This species shows an interesting sex role reversal between seasonal forms that  
98 develop at different temperatures, and where temperature cues in the arrival of different seasons.

99 In particular, wet season (WS) males, reared at high temperatures, play the active courting role,  
100 while DS males, reared at low temperatures, do much less courtship and become, instead, the  
101 choosy sex (16). The adaptive reason driving courtship plasticity in males is associated with  
102 increased reproductive costs for DS males, which provide females with beneficial  
103 spermatophores (16). Provision of this spermatophore ultimately shortens DS male lifespan, but  
104 lengthens DS female lifespan and helps them survive through the more stressful and resource-  
105 limited dry season (15, 16). While the behavioral ecology of these butterflies may explain  
106 seasonal variation in male courtship rates, the neural re-wiring that switches the male behavior is  
107 completely unknown.

108

109 In *B. anynana*, signaling of the hormone 20-hydroxyecdysone (20E) during early pupal  
110 development has been shown to regulate male courtship (17). In DS males, throughout pupal  
111 development, there are significantly lower levels of 20E titers circulating in the hemolymph than  
112 in WS males (17). The reduced courtship of DS males, however, can be switched to the WS  
113 active courting form by rearing pupae at higher temperatures during the first 50% of pupal  
114 development (15) or, alternatively, by keeping the pupae at low temperatures but injecting them  
115 with 20E at 30% of pupal development (17). These experiments suggest that this pupal stage is a  
116 critical period that determines male sexual behavior and that 20E may play an organizing role in  
117 the developing male brain of *B. anynana*. However, we currently have no direct evidence that  
118 20E acts specifically on the brain to alter expression of genes that regulate male courtship  
119 behavior in adults. High levels of 20E could upregulate genes required for active courtship such  
120 as those described for *Drosophila* including *fruitless*, *doublesex* and *yellow* (9, 18, 19).

121 Alternatively, 20E signaling may not lead to appreciable differences in the neural circuitry of dry  
122 and wet season male brains, but may instead influence other phenotypic traits that are also  
123 important in courtship behavior such as pheromone production (20) or the UV brightness of  
124 eyespot centers (16).

125

126

127

128

129

## 130 **Results**

131

132 *Genes involved in melanin synthesis, dopamine metabolism and JH signaling are differentially*  
133 *expressed in pupal brains*

134 To evaluate the direct organizational effects of 20E on the pupal brain of *B. anynana* males, and  
135 identify changes in gene expression levels that could impact the future sexual behavior of males,  
136 we compared the transcriptome of DS male brains injected with 20E at 30% pupal development  
137 (referred to as DS20E thereafter) with DS and WS male brains injected with a vehicle solution at  
138 the same developmental stage (DSV and WSV, respectively) (Fig. 1). RNA-seq extractions  
139 yielded a total of  $2.11 \times 10^8$  raw reads from 12 RNA-seq libraries. All read data was used to  
140 produce a transcriptome comprising of 1,403,420 total Trinity transcripts and 689,657 Trinity  
141 genes with an N50 length of 973 (full summary statistics are provided in Table S1 and Fig. S1).  
142 Mapping of the raw reads back to the transcriptome revealed that the overall alignment rate was  
143 98.83-98.98%. Processing the transcriptome through CD-HIT (21) identified 1,045,896 unigenes  
144 in the transcriptome at 0.95 similarity. We identified 399 differentially expressed genes (DEGs)  
145 between DSV and WSV pupal brains, 302 were upregulated and 97 were downregulated in DSV.  
146 Comparing DS20E pupal brains to WSV, we identified 399 DEGs, 291 were upregulated and  
147 108 were downregulated in DS20E. Comparing DS20E pupal brains to DSV we identified 151  
148 DEGs, 79 were upregulated and 72 were downregulated in DS20E. Overall, the smaller number  
149 of differentially expressed genes observed between DSV and DS20E (151) compared to DSV  
150 and WSV (399) suggest that the DS20E brain transcriptome profile was more similar to DSV  
151 than WSV at 2 hours post-injection (Fig. S2 heat map). The full list of DEGs can be found in  
152 Table S2.

153

154 Genes known to be important in male courtship behavior such as *fruitless* and *doublesex* (22) were  
155 not differentially expressed at 30% of pupal brain development. However, the melanin pathway  
156 gene *yellow* was upregulated in both DSV and DS20E when compared to WSV. We also found  
157 that *dopamine N-acetyltransferase* (AANAT1/DAT1) was upregulated in DS20E (but not in DSV)  
158 when compared to WSV. Other potential genes of interest pertaining to courtship behavior  
159 included *Juvenile hormone* (JH), which was downregulated in DSV compared to WSV, and  
160 *Juvenile hormone epoxide hydrolase-like* (which hydrolyses JH) was upregulated in DSV and  
161 DS20E when compared to WSV. Genes involved in neural development included *neuropeptide*

162 *CCHamide2*, *Neural Wiskott-Aldrich syndrome protein* and *lethal 2 essential for life l(2)efl*. These  
163 genes were downregulated in DSV compared to WSV with *l(2)efl* also downregulated in DS20E  
164 compared to WSV. Fig. 2 summarizes the log-fold change values and *p*-values of the top 10  
165 annotated DEGs. See table S3 for a descriptive list of the DEGs associated with neural  
166 development.

167

### 168 *20E downregulates the expression of yellow 4h after injections*

169 From the transcriptomics analyses, we did not identify interesting candidate genes with a  
170 regulation pattern consistent with the high courtship of WSV and DS20E injected males, and the  
171 low courtship of DSV males. We thus decided to explore further the pupal brain expression of  
172 *yellow* because it was previously shown to affect courtship behavior in *Drosophila melanogaster*  
173 (18, 23) and was found to be upregulated in both DS treatments compared to WS. We hypothesized  
174 that 20E may affect *yellow* expression at a later stage post injection, impacting the courtship  
175 behavior in adults. To confirm the regulation of *yellow* expression by 20E in male pupal brains,  
176 we used qPCR to measure the relative expression of *yellow* in the brains of developing pupae at 3  
177 different time points after injections of the hormone. Similar to the transcriptomics experiment,  
178 we injected 20E in DS male pupae at 30% development, and a vehicle solution in both DS and WS  
179 pupae at the same stage, and assessed the relative levels of *yellow* in dissected pupal brains at 2,  
180 4, and 24 hours post injection.

181

182 Two hours post-injection, the levels of *yellow* were about 2.5 times higher in pupal brains of both  
183 DSV and DS20E compared to the level of expression in WSV pupal brains, (mirroring our RNA-  
184 seq results), although the expression levels were not significantly different (Fig. S3, ANOVA:  $F$   
185 = 0.50,  $p = 0.62$ ). However, at 4 hours post-injection, the expression of *yellow* increased  
186 significantly by about 8-fold in DSV compared to WSV pupal brains (Fig 3, ANOVA:  $F = 5.43$ ,  
187  $p = 0.023$ ; post-hoc analysis WSV-DSV: adj.  $p = 0.027$ ), while the level of *yellow* expression in  
188 DS20E remained low, similar to those of WSV brains (ANOVA post-hoc analysis WSV-DS20E:  
189 adj.  $p = 0.79$ ). Twenty-four hours post-injection, expression levels of *yellow* in the pupal brains  
190 of DSV and DS20E were respectively 2.8 and 3.7 times higher than in WSV (Fig. S3). Relative  
191 levels of *yellow* expression were significantly higher in DS20E than in WSV pupal brains  
192 (ANOVA:  $F = 4.12$ ,  $p = 0.046$ ; post-hoc analysis WSV versus DS20E: adj.  $p = 0.046$ ). These

193 results demonstrate that a single injection of 20E into DS pupae at 30% of development was  
194 sufficient to decrease *yellow* expression levels in DS20E to WSV levels at 4 hours post-injection.  
195 This single injection did not impact *yellow* levels at the earlier 2hr time period, nor keep *yellow*  
196 levels low at 24 hours post injection, suggesting that a short interval of time around 30% pupal  
197 development encompasses a hormone-sensitive window in which *yellow* is downregulated by  
198 20E to WS levels.

199

#### 200 *Yellow mutant males courted more frequently and for a longer duration than Wt males*

201 We hypothesized that Yellow may be a repressor of male courtship as DS males exhibit lower  
202 courtship than WS males and have significantly higher expression of *yellow* during pupal brain  
203 development. To test this hypothesis, we generated a Yellow mutant homozygous line in *B.*  
204 *anymana* to investigate if loss of Yellow function leads to elevated levels of courtship in DS males  
205 alone or in both DS and WS males (Fig. S4). Using this Yellow knockout (KO) line, we compared  
206 the duration and frequency of the Yellow mutant and the wildtype (Wt) male courtship sequence,  
207 including copulation. Yellow mutant males courted for a longer duration (WS:  $t = 2.181$ ,  $p =$   
208  $0.0323$ ; DS:  $t = 2.083$ ,  $p = 0.0416$ ; Fig. 4a) and more frequently (WS:  $z = 4.165$ ,  $p < 0.0001$ ; DS:  
209  $z = 2.629$ ,  $p = 0.00855$ ; Fig. 4b) than Wt males regardless of seasonality. In addition, DS Yellow  
210 mutant males remained in copulation longer ( $t = 2.174$ ,  $p = 0.039$ ; Fig. 4c) than DS Wt males.

211

212 Because Yellow males have a lighter overall pigmentation, despite being identical in the brightness  
213 of a known sexual ornament, the eyespot's ultraviolet reflecting white center on the ventral and  
214 dorsal sides of the forewing (Fig. S5) (24, 25), we repeated these male courtship observations using  
215 decapitated females. Decapitation prevents important visual cues detected by a female from  
216 impacting a male's behavior, such as more intense courtship provoked by a female's increased  
217 rejection behavior (26). Yellow mutant males still courted for a longer duration (WS:  $t = 2.083$ ,  $p$   
218  $= 0.0416$ ; DS:  $t = 2.269$ ,  $p = 0.0266$ ; Fig. 4a) and more frequently (WS:  $z = 10.59$ ,  $p < 0.0001$ ; DS:  
219  $z = 8.246$ ,  $p < 0.0001$ ; Fig. 4b) than Wt males regardless of seasonality (see also Fig. S6). This  
220 result indicates that Yellow alters male courtship behavior independently of the female's behavior  
221 towards those males.

222

223



224 *Yellow mutant males courted more frequently and copulated longer in their DS form than WS form*

225 To test whether differences in Yellow expression levels were sufficient to explain courtship  
226 differences between the seasonal forms, we compared the amount of courtship between DS and  
227 WS Yellow mutant males. If Yellow, alone, was responsible for courtship differences between the  
228 forms then DS and WS Yellow mutant males should display similar levels of courtship. DS Yellow  
229 mutant males courted live females more frequently ( $z = 2.324$ ,  $p = 0.0201$ ; Fig. 4b) and copulated  
230 longer ( $t = 2.174$ ,  $p = 0.039$ ; Fig. 4c) than WS Yellow mutant males. Similar behavior was  
231 observed in males courting decapitated females, with DS Yellow mutant males courting more  
232 frequently ( $z = 2.454$ ,  $p = 0.0141$ ; Fig. 4b) and copulating longer ( $t = -2.34$ ,  $p = 0.032$ ; Fig. 4c)  
233 than their WS counterparts.

234

235

## 236 **Discussion**

237 In insects, hormones are typically assumed to regulate sexual behavior by activating existing  
238 neural circuits that control processes such as sexual maturation, memory formation and  
239 pheromone communication (11, 27-29). Recently, it has been shown that hormones can also  
240 regulate sexual motivation by repressing activation of existing neural circuits (5). It remained  
241 unclear, however, whether exposure to different levels of hormones earlier in development could  
242 organize neural circuits that affect sexual behavior in adults. Here, we provide evidence that the  
243 ecdysteroid 20E plays an organizational role during pupal brain development in *B. anynana* by  
244 repressing expression of the *yellow* gene which leads to seasonal differences in male courtship  
245 behavior.

246

247 *Yellow is regulated by 20E during pupal brain development and functions a repressor of male*  
248 *courtship in B. anynana*

249 We show that *yellow* is significantly upregulated in the pupal brains of DS male butterflies which  
250 court less than WS males. This increase in *yellow* expression appears to be in response to  
251 seasonal fluctuations in 20E, as injection of this hormone into DS males at 30% of pupal  
252 development was sufficient to suppress *yellow* expression to levels observed in WS pupal brains  
253 at 4 hours post-injection, as well as to rescue WS courtship levels in adults (17). These results  
254 suggest that this period encompasses a critical window during brain development which is  
255 sensitive to circulating levels of 20E. High levels of *yellow* in DS males suggested that *yellow*  
256 was a repressor of courtship. This was confirmed by knocking out *yellow* in *B. anynana* and  
257 observing male Yellow mutants exhibiting increased courtship frequency and duration compared  
258 to wildtype males of both seasonal forms. Given that Yellow WS mutants displayed more active  
259 courtship than wildtype WS males, this suggests that low levels of *yellow* expression are still  
260 required in wildtype WS males to reduce courtship and optimize energy expenditure, as  
261 increased wing fluttering observed in the Yellow KO line did not translate to increased mating  
262 success.

263

264 Comparing the behavior of Yellow mutant males between seasonal forms produced additional  
265 insights into the role of *yellow* in regulating male courtship plasticity. The complete loss of *yellow*  
266 led to DS males courting more than WS males. This result was surprising as it suggests that

267 removal of Yellow inverts the relative amount of courtship performed by WS and DS males; It  
268 leads DS males to court more than WS males. This suggests that Yellow is required for inverting  
269 a biased level of courtship that would take place in these butterflies driven by temperature alone.  
270 Without the action of *yellow*, males reared at high temperature during development would court  
271 less than males reared at low temperatures. This indicates that the high levels of *yellow* expression  
272 in the brains of DS males is absolutely essential to produce the low levels of courtship in this  
273 seasonal form, and that other factors controlled by rearing temperature and by 20E are biasing  
274 adult courtship levels in the opposite direction to those observed in wildtype individuals. These  
275 factors can be explored in future.

276

277 Our findings are in striking contrast to those observed in *Drosophila* where *yellow* is required for  
278 normal male courtship behavior. Exactly how *yellow* expression influences male courtship  
279 behavior in *Drosophila* has been a topic of investigation that has yielded conflicting results. An  
280 early study suggested that *yellow* mutant males were less successful during courtship and  
281 displayed reduced wing vibrations (30). Further tests of these observations showed that  
282 mutations in *yellow* disrupted wing extension during the courtship ritual, preventing males from  
283 performing a courtship song which is required for male mating success (18, 31). However, recent  
284 work by Massey et al. argued that a lack of melanization in the sex combs of *yellow* mutants,  
285 rather than any impairment in neural circuitry affecting courtship song, was the trait that  
286 prevented males from successfully grasping females (19), an idea that was proposed earlier (32).  
287 It is possible that the fly laboratory stock might have evolved between the earlier and the later  
288 experiments, as the courtship observations repeated by Massey et al., produced different results  
289 from the original observations on the same stock (30). All research to date on *yellow* mutants in  
290 *Drosophila*, however, clearly demonstrate that *yellow* is absolutely required for successful male  
291 courtship.

292

293 *yellow may influence courtship behavior in B. anynana via the dopaminergic signaling pathway*

294 Dopamine is an important catecholamine neurotransmitter which regulates a variety of behaviors  
295 including motor output, drive, arousal, pleasure and memory (33, 34). Dopaminergic signaling  
296 has been shown to regulate not only mating drive but also persistence and duration of mating in  
297 male *Drosophila* (35, 36). Melanin synthesis enzymes are expressed in the *Drosophila* brain and

298 may be involved in the production of neuromelanin in dopaminergic neurons (37). Yellow is  
299 thought to function as a dopachrome conversion enzyme (DCE) in the melanin pathway  
300 converting L-Dopa to Dopa-melanin (38, 39). L-Dopa is also used as substrate for dopamine  
301 which is involved in both cuticle pigmentation and neurotransmission (36). Thus, variation in  
302 *yellow* expression could alter the availability of L-Dopa for dopamine synthesis, with higher  
303 expression of *yellow* in DS brains leading to reduced L-Dopa. Alternatively, Yellow may  
304 physically bind to dopamine, as demonstrated in a study of salivary proteins in sandflies (40).  
305 Thus, the increased expression of *yellow* in DS brains could lead to a reduction in dopamine  
306 availability, which may inhibit courtship behavior. In Fig. 5, we suggest a possible mechanism of  
307 Yellow involvement in the pathway converting tyrosine to L-Dopa in dopaminergic neurons.

308  
309 Currently we have no direct evidence that dopamine levels differ between DS and WS *Bicyclus*  
310 brains. However, the expression profile of a few genes in our transcriptome analyses may  
311 provide some indirect evidence. We found that dopamine N-acetyltransferase, AANAT/DAT1  
312 was upregulated in pupal brains of DS20E (but not in DSV) as compared to WSV brains. This  
313 may indicate a transient response to the 20E injection. The function of AANAT is to metabolize  
314 and inactivate secreted dopamine in the synapse shortly after release (33, 37). In young female  
315 *Drosophila virilis*, higher titers of 20E leads to an increase in dopamine, although this appears to  
316 be associated with reduced activity of AANAT (41). However, in retinal cells of fish, AANAT  
317 activity is positively correlated with dopamine levels (42). An increase in dopamine induced by  
318 20E would provide a mechanistic explanation as to why DS male pupa injected with 20E display  
319 active WS courtship behavior. Functional experiments measuring or manipulating dopamine  
320 levels, however, are required to test the hypothesis that dopamine levels are higher in WS male  
321 pupal brains.

322  
323 We also observed changes in Juvenile hormone (JH) signaling, which is known to interact with  
324 dopamine to affect sexual maturity and courtship behavior in *Drosophila*, likely through changes  
325 in neural development (14, 43). In DS pupal brains, JH was downregulated and Juvenile  
326 hormone epoxide hydrolase (JHE), which degrades JH (44), was upregulated. These findings  
327 could indicate that dopamine levels are low in DS male pupal brains as dopamine increases JH  
328 titers in young female *D. virilis* by inhibiting its degradation (45). JH is also associated with

329 increased dopamine levels in male honeybees (46). Although we also see an upregulation of JHE  
330 but no longer a downregulation of JH in DS20E, this may reflect a response to changing levels of  
331 dopamine. Interactions between 20E, JH, dopamine and AANAT in *Drosophila* represent a  
332 complex pathway as depicted in (41, 47) thus, we must interpret our findings with caution.  
333 However, given that this is an important pathway for regulating courtship behavior in  
334 *Drosophila*, the differential expression of these genes in our transcriptome analyses suggest their  
335 possible involvement in regulating courtship behavior in *B. anynana*.

336

### 337 *Drosophila* courtship genes do not impact *Bicyclus* courtship behavior at this pupal stage

338 A number of genes that are known to be important for male courtship in *Drosophila* (*fruitless*,  
339 *dsx crol*, *lola*, *cadN* and *chinmo*) (22), were surprisingly not differentially expressed between any  
340 of our treatment groups and all showed very low levels of expression (Fig. 2). Thus, it appears  
341 that in *B. anynana* these genes do not influence neural re-wiring occurring at this particular stage  
342 of brain development. However, we cannot exclude the possibility that these genes are  
343 upregulated at a later time point after the 20E injection. We did, however, identify some other  
344 differentially expressed genes including *Neural Wiskott-Aldrich syndrome protein* (N-WASP),  
345 *CCHamide2* and *lethal 2 essential for life (l(2)efl)* that may be important in neural development  
346 and behavior and could serve as interesting candidates for future studies (see Table S3).

347

## 348 **Conclusions**

349 Here, we show that male DS butterflies court less than WS butterflies due to temperature-induced  
350 changes in levels of 20E, which alter the expression of the *yellow* gene during pupal brain development  
351 leading to differences in adult courtship behavior. In *B. anynana*, *yellow* functions as a repressor of male  
352 courtship and is a downstream target of 20E. Our results suggest potential interactions of 20E on JH and  
353 dopamine signaling, a circuit that is well described in *Drosophila*. Future studies examining dopamine  
354 levels between the seasonal forms and the individual role of 20E and JH on dopaminergic signaling  
355 would help clarify mechanistically why the *yellow* gene functions as a repressor of male courtship in  
356 these butterflies. We propose an organizational role for 20E, suggesting convergence in hormone  
357 regulation of sexual behavior in insects and vertebrates. For animals living in seasonal environments,  
358 selection may favor adaptations that use external cues to optimize behavior, such as employing

359 environmentally induced hormones like 20E to organize neural circuits during critical windows of brain  
360 development.

361

### 362 **Acknowledgements**

363 We would like to acknowledge Dong Qiang Cheng, for helping EJT with the hardware issues on  
364 lab server; Jan Gruber, for advising EJT with the Linux operating system and also Firefly Farms  
365 in Singapore for supplying corn for larval rearing.

366

### 367 **Funding**

368 EJT was supported by a Postdoctoral Fellowship from Yale-NUS College. We thank NSF award  
369 DDIG IOS-1110523 to AM and AB, Ministry of Education Singapore, award MOE2018-T2-1-  
370 092 to AM, and National Research Foundation, Singapore, Investigatorship award NRF-  
371 NRFI05-2019-0006 to AM.

372

373

374

375 **Methods**

376

377 **Transcriptome assembly and analyses**

378

379 *Sample collection and Illumina(R) RNA-seq experiments*

380

381 To mimic dry and wet season conditions, caterpillars of *B. anynana* were reared under WS and DS  
382 temperatures in climate-controlled rooms at 27°C and 17°C, respectively, at 80% humidity, and a  
383 12:12 hr light:dark photoperiod. Caterpillars were fed corn plants *ad libitum* until pupation. Pupae  
384 were staged, such that the percent of pupal development was known for all individuals. At 30% of  
385 pupal development (day 2 in the WS butterflies and day 6 in the DS butterflies) DS pupae were  
386 injected with either 3 µl of 2000 pg/µl (6000 pg total) (10% 20E in EtOH + 90% saline) of 20E  
387 (Sigma-Aldrich®) or with 3 µl of vehicle (10% EtOH and 90% saline) and WS pupae were injected  
388 with 3 µl of vehicle in the lateral posterior region of the fifth abdominal segment. The injections  
389 were done at 1200 h and the brains were dissected two hours later, at 1400 h. We chose to inject  
390 the animals two hours before collection in order to give the 20E time to circulate through the open  
391 circulatory system of the insect to reach the brain and to affect gene expression in this tissue. We  
392 chose this time point after injection to collect the samples because previous studies have  
393 demonstrated that genes, which respond early to 20E signaling are expressed about 2 hours after  
394 exposure to 20E (48, 49).

395

396 Samples from each treatment were collected on each collection day in order to reduce the  
397 confounding effects of day of collection on gene expression. Each sample consisted of three  
398 biological replicates of wet season pupal brains following treatment with vehicle only; four  
399 biological replicates of dry season pupae treated with vehicle only; and five biological replicates  
400 of dry season pupae treated with 20E. Each biological replicate was made up of mRNA pooled  
401 from the brains of five different individual male pupae. Brains were pooled to account for the  
402 genetic variation in the colony. The pupal brains were dissected in a solution of ice cold 1X PBS.  
403 After each dissection, the brain was immediately immersed in a 1.5 eppendorf tube containing 500  
404 µl of TRIzol® reagent (Life Technologies®) and 3 RNase-free beads (#SSB14B 1.4mm Stainless  
405 Blend NEXT>>>ADVANCE®).

406

407 Once all five brains from a particular treatment group were placed in the TRIzol reagent, the brains  
408 were immediately homogenized using a Bullet Blender (NEXT>>>ADVANCE®) for three  
409 minutes and total RNA was extracted using the trizol-chloroform protocol. DNA was removed  
410 using gDNA Eliminator Mini Spin Columns from the RNeasy Plus Micro Kit (Qiagen®) and  
411 following the kit instructions. The quality of the extracted RNA was checked using a ND1000  
412 spectrophotometer (NanoDrop® Technologies) and stored at -80°C. The samples were submitted  
413 to the W.M. Keck Biotechnology Resource Laboratory for Illumina® RNA-Seq. The RNA  
414 samples consisted of 4 µg of total RNA in 20 ml of water, and was run on a separate lane of a flow  
415 cell on a HiSeq2000. The Keck Biotechnology Resource processed the samples following standard  
416 Illumina® RNA-Seq protocol.

417  
418 *Transcriptome assembly*

419 We assembled the transcriptome from a total of 12 RNA-Seq libraries. Raw reads of the RNA-seq  
420 libraries were uploaded to the SRA database with the SRA accession number PRJNA544388.  
421 Prior to performing the transcriptome assembly, we performed quality trimming of the input raw  
422 reads using Trimmomatic using the default options (50). We assembled a de novo transcriptome  
423 using Trinity 2.4.0 (51) and Bowtie2, following the protocol by Haas et al. (52). The transcriptome  
424 was then uploaded to the Transcriptome Shotgun Assembly (TSA) Database, following the TSA  
425 guidelines. During this process, transcripts were screened for vector contaminations and any vector  
426 and linker sequences were removed. In addition, transcripts smaller than 200 bp were screened  
427 and removed from the assembly. This Transcriptome Shotgun Assembly project has been  
428 deposited at DDBJ/EMBL/GenBank under the accession GHRJ00000000. The version described  
429 in this paper is the first version, GHRJ01000000.

430  
431 To characterize the quality of our transcriptome assembly, we used scripts in the Trinity toolkit.  
432 First, we computed assembly statistics, which is the contig N50 value based on the set of transcripts  
433 representing 90% of the expression data, using the TrinityStats.pl script. These assembly statistics  
434 for *B. anynana* brain transcriptome are reported in Table S1. Next, we computed the N50 statistics  
435 of the top most highly expressed transcripts that represent x% of the total normalized expression  
436 data, using the contig\_ExN50\_statistic.pl script. The N50 statistics are presented in Figure S1. To  
437 assess the proportion of raw reads mapped to the transcriptome assembly, we used Bowtie2. We



438 then extracted transcripts that are most differentially expressed and clustered these transcripts  
439 according to their patterns of differential expression using the `analyze_diff_expr.pl` script from the  
440 Trinity toolkit. The clustering analysis indicated that the biological replicates from the same  
441 treatment clustered together, as shown in Figure S2.

442  
443 Next, we obtained unigenes for the transcriptome using CD-Hit version 4.6 (21) with similarity  
444 set to 0.95. CD-Hit clustered all sequences with similarity  $\geq 95\%$ , retaining only the longest  
445 transcript, thus splice variants/isoforms were removed and redundancy was reduced. The  
446 transcriptome assembly with unigenes was then used for differential gene expression, described in  
447 the next section.

448  
449 *Differential gene expression*

450 To estimate transcript abundance, we used RSEM 1.3.2 (53), a software which uses Bowtie2 (54)  
451 to align the transcripts to the transcriptome assembly, thus quantifying gene and isoform  
452 abundances. The RSEM output reported normalized expression metrics as fragments per kilobase  
453 transcript length per million fragments mapped (FPKM) and transcripts per million transcripts  
454 (TPM). Next, we used edgeR 3.28.1 (55), to examine differential expression of genes across the  
455 three treatments (DSV vs WSV, DS20E vs DSV and DS20E vs WSV). EdgeR normalizes RNA  
456 composition by finding a set of scaling factors for the library sizes that minimize the log-fold  
457 change ratios (logFC) between the samples for most genes. We used the default method in edgeR  
458 for computing these scale factors, which is a trimmed mean of Mvalues (TMM) between each pair  
459 of samples. Genes with a False Discovery Rate (FDR) of  $<0.05$  and logFC of  $\geq 2$  were defined as  
460 differentially expressed genes (DEGs).

461  
462 In order to understand the DEGs induced by the hormone treatment, we further annotated the DEGs  
463 with Blast2GO 5.2.5. We used the public NCBI Blast service (QBLAST) to blast our sequences  
464 against the non-redundant protein database using the `blastx-fast` program. Matched transcripts  
465 were filtered using a cut-off E-value of  $1 \times 10^{-3}$ ; otherwise the default settings for Blast2GO were  
466 used at each step. To annotate the remaining transcriptome, we performed a local `blastx` of the  
467 assembled contigs against the *Bicyclus anynana* v1.2 draft genome (56). The annotated  
468 transcriptome has been deposited on Dryad and will be made available for publication.

469 *qPCR sample collection and experiments*

470 Sample collection was similar to the one described above for the RNA seq experiment. We  
471 measured the total development time of Wt pupae, and at 30% development (2.5 and 6.5 days for  
472 WS and DS pupae respectively in these rearing conditions), we injected pupae with 20E or vehicle  
473 solutions using the same protocol as described above. Pupal brains were dissected 2 hours, 4 hours  
474 and 24 hours after injections in ice cold 1X PBS, placed immediately into RNALater (Qiagen,  
475 GmbH, Hilden, Germany) and stored at -20°C until RNA extraction. We used 5 biological  
476 replicates per treatment, each made of 5 pooled brains (for the 2 hours dissections) or 2 pooled  
477 brains (for the 4- and 24-hour dissections).

478

479 Total RNA extraction, including the elimination of genomic DNA, was done using the Qiagen  
480 RNeasy Plus Mini Kit (Hilden, Germany) following the manufacturer's instructions.  
481 Complementary DNA was synthesized using the RevertAid RT Reverse Transcription Kit  
482 (Themoscientific). 10 ng of cDNA were used for qPCR with the KAPA SYBR FAST qPCR Kit  
483 (KK4604, KAPA Biosystems, Wilmington, MA, USA) and the experiment run on the Biorad  
484 CFX96 system using the TqPCR protocol described in Zhang et al. (57). Primer efficiencies were  
485 calculated using 0.5, 5 and 50 ng of cDNA from Wt tissue (with 3 technical replicates). The primers  
486 are described in Table S4.

487

488 We calculated the relative transcript levels using the common based method (58). The Ct values  
489 were normalized to the reference gene *EFl $\alpha$*  and to the average Ct of the WS reference samples.  
490  $\Delta$ Ct values from each treatment were compared using a one-way analysis of variance (ANOVA)  
491 followed by a post-hoc analysis providing p values adjusted with the Tukey method. Statistical  
492 analyses were performed in R v.4.0.0 (59) implemented in RStudio v.1.2.5042 (60), using Rmisc,  
493 car and emmeans packages (61-63).

494

495 *Generation of CRISPR-attP Yellow knock out line*

496 To establish a Yellow mutant line we inserted an attP sequence into exon 4 of the *yellow* gene to  
497 disrupt its overall sequence (Fig S7). We used a knock-in method through homology directed  
498 repair (HDR) using a single-stranded DNA (ssDNA) as a template. The ssDNA construct was  
499 made following methods described in (64). The ssDNA contains 66 bp and 60 bp of homologous

500 sequence around the target region on each side of the attP sequence motif. We injected 500 ng/ $\mu$ l  
501 of a sgRNA targeting the *yellow* gene, 500 ng/ $\mu$ l Cas9 mRNA, and 160 ng/ $\mu$ l ssDNA into fertilized  
502 2-3 hr old embryos. Out of 254 injected embryos, 87 larvae hatched, resulting in 14 adults (6 males  
503 and 8 females). We then crossed 3 G<sub>0</sub> mosaic butterflies (showing some yellow patches of  
504 coloration on the wings) with 3 Wt to obtain the G<sub>1</sub> generation. To identify which cage contained  
505 transgenic butterflies with the attP insertion, we pooled 30 embryos from each cage, extracted  
506 genomic DNA, and performed PCR. One out of 3 cages showed a positive band. In cages that were  
507 identified as contained transgenic individuals we performed further genotyping of individual  
508 larvae using haemolymph PCR (Fig. S7). We isolated 5 transgenics out of 102 G<sub>1</sub> genotyped  
509 animals. We confirmed that the PCR amplicon flanking the gRNA target site was the expected  
510 sequence although it contained 2 substitutions outside the attP sequence (Fig. S7). We crossed  
511 these 5 positive G<sub>1</sub> butterflies with a Yellow phenotype with Wt counterparts, and then identified  
512 heterozygous G<sub>2</sub> mutant offspring by haemolymph PCR since *B. anynana yellow* gene is likely a  
513 dominant gene regarding its effect on body color. We further crossed heterozygous G<sub>2</sub> butterflies  
514 with each other, and obtained a homozygous G<sub>3</sub> generation using, again, genotyping via  
515 haemolymph PCR.

516

## 517 **Behavioral Assays**

### 518 *Animal husbandry*

519 Larvae from both the Yellow CRISPR-attP line and Wt were fed with young maize plants (*Zea*  
520 *mays*) and adults with mashed bananas *ad libitum*. Larvae of both lines were reared in WS and DS  
521 conditions as described above. Prior to eclosion (Day 0), pupae were separated according to their  
522 sex to ensure virginity. Adults that emerged on the same day were then transferred to other cages  
523 and dated accordingly.

524

### 525 *Behavioral experiments*

526 Behavioral assays were conducted in cylindrical hanging cages (30cm x 40cm) under one full  
527 spectrum light tube (Plantmax) and one UV light bulb (Arcadia Marine Blue), at 23°C, from 17:00  
528 to 18:00. This specific time of observation was chosen because *B. anynana* exhibits crepuscular  
529 courtship (17). Visual barriers were placed between cages to prevent mate-copying (65). Within  
530 each sex, butterflies used for each assay were of the same age. All butterflies used in the assays

531 ranged from four to eight days old. Two experiments were performed, one with live females and  
532 the other with decapitated females. The treatments were i) two Wt males x two Wt females, and  
533 ii) two Yellow mutant males x two Wt females (Fig. S4). One of the two males/ females in an  
534 assay was dotted with a black marker at both of its ventral hindwings to allow for sex-specific  
535 scoring of behavior. The multiple elements of courtship, as documented in Nieberding et al. (66),  
536 were scored in the assays: 1) localization (flying to other butterfly), 2) rapid flickering of wings,  
537 3) thrusting (touching female's wings with head), and 4) attempting (curling of the abdomen) (Fig.  
538 S4). Orientation (orienting body to female's posterior) was not recorded since it was difficult to  
539 score or interpret their intent (courtship or coincidence) with that behavior. Latency to mate (time  
540 taken from the start of assay to the first mating) and mating duration were recorded as well.  
541 Behavioral assays lasted one hour, and quantification of an individual male behavior stopped once  
542 the first mating had occurred (i.e. even if one has mated, the other male's behavior is still quantified  
543 until its own mating or one hour has lapsed).

544  
545 For decapitation experiments, only females were decapitated to characterize male sexual behavior  
546 in the absence of female response (26). The same behavioral scoring as described above was used  
547 for this experiment. Decapitated females were first anesthetized in a -20°C freezer for 20 minutes  
548 and their heads were removed. Females were pinned through their thorax into opposite sides of the  
549 cage as illustrated in Fig. S4c and d. Based on personal observations, males tend to begin courtship  
550 when females start moving or signal readiness. Without movement, which was observed in some  
551 of the decapitation assays, males do not attempt to court at all, regardless of treatment type.  
552 Therefore, to overcome this potential issue, the pins (and therefore the thorax) of decapitated  
553 females were moved gently to emulate movement after 30 minutes had passed since the start of  
554 the assay. This specific timepoint was used as the average mating latency for live experiments was  
555 approximately 30 minutes. Thus, this reduces bias as much as possible, while still managing to test  
556 the effect of the *yellow* gene in male courtship behavior.

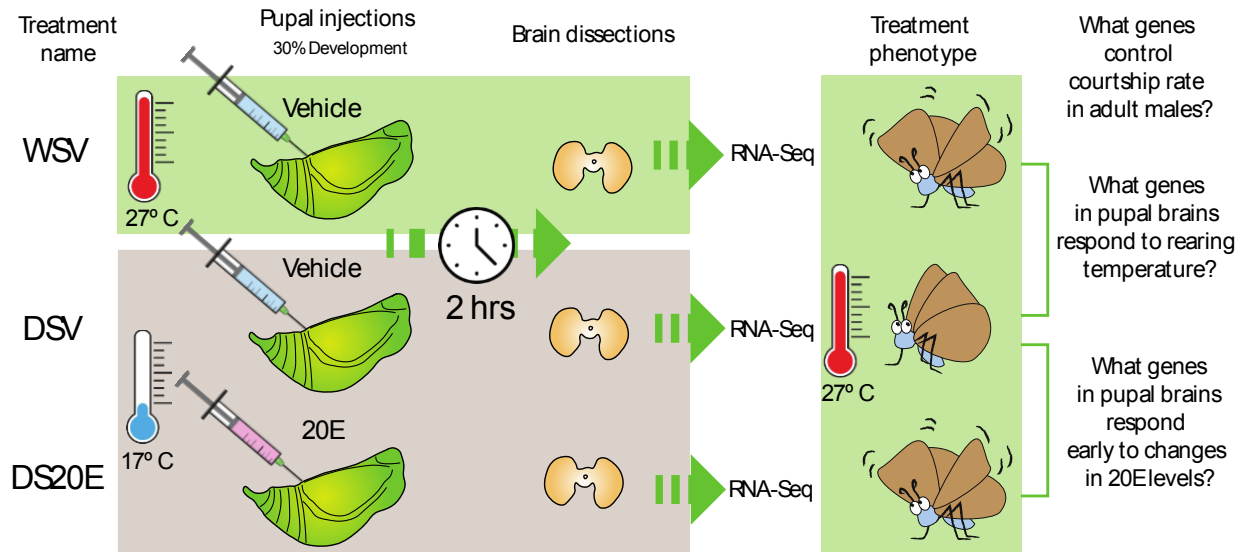
### 557 558 *Statistical analysis*

559 The data was evaluated for equality of variances and normality using the Levene's test and  
560 Shapiro-Wilk test, respectively. Total duration and frequency of courtship were calculated by  
561 adding up the duration/ frequency of all the courtship elements displayed (localising + flicker +

562 thrust + attempt) during the observation period. A Generalised Linear Model (GLM) with a  
563 Tweedie distribution (Gamma family; tweedie package (67)) was done to test the impact of the  
564 treatment type (Yellow/ WT) and season (WS/ DS) on the total duration of courtship. A Tweedie  
565 distribution (Gamma) was used due to the high number of zeroes and the skewness of data. The  
566 impact of the treatment type (Yellow/ WT) and season (WS/ DS) on the frequency of each  
567 courtship element was compared using a Zero- Inflated Poisson Model (pscl package (68)). Both  
568 mating latency and mating duration of the mated pairs were compared using independent t- tests.  
569 Chi-square tests were carried out to identify any associations between treatment type and mating  
570 success. Statistical tests and figures were done with IBM SPSS Statistics 25 and R-4.0.2 (59). The  
571 spectral data of eyespots was visualized using the pavo package (Fig. S5 (69)). Spectral analysis  
572 was done through calculating area under curve (AUC) for each eyespot replicate and the AUC  
573 analyzed using an ANOVA with post-hoc Tukey test in R.  
574

575 **Figures**

576



577

578

579

580

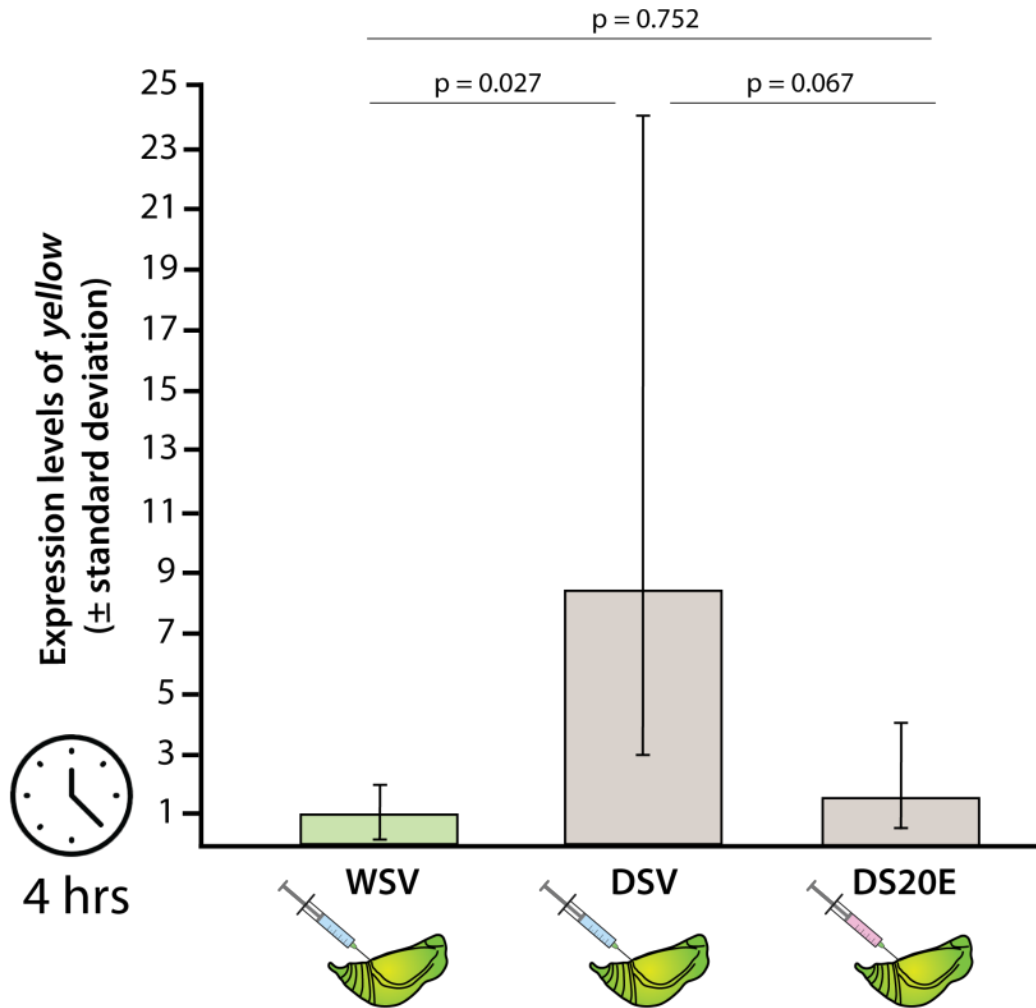
581

582

**Fig. 1.** Overview of the experimental set-up for the pupal injections, brain dissections and RNA-seq for the three different treatment groups.



597



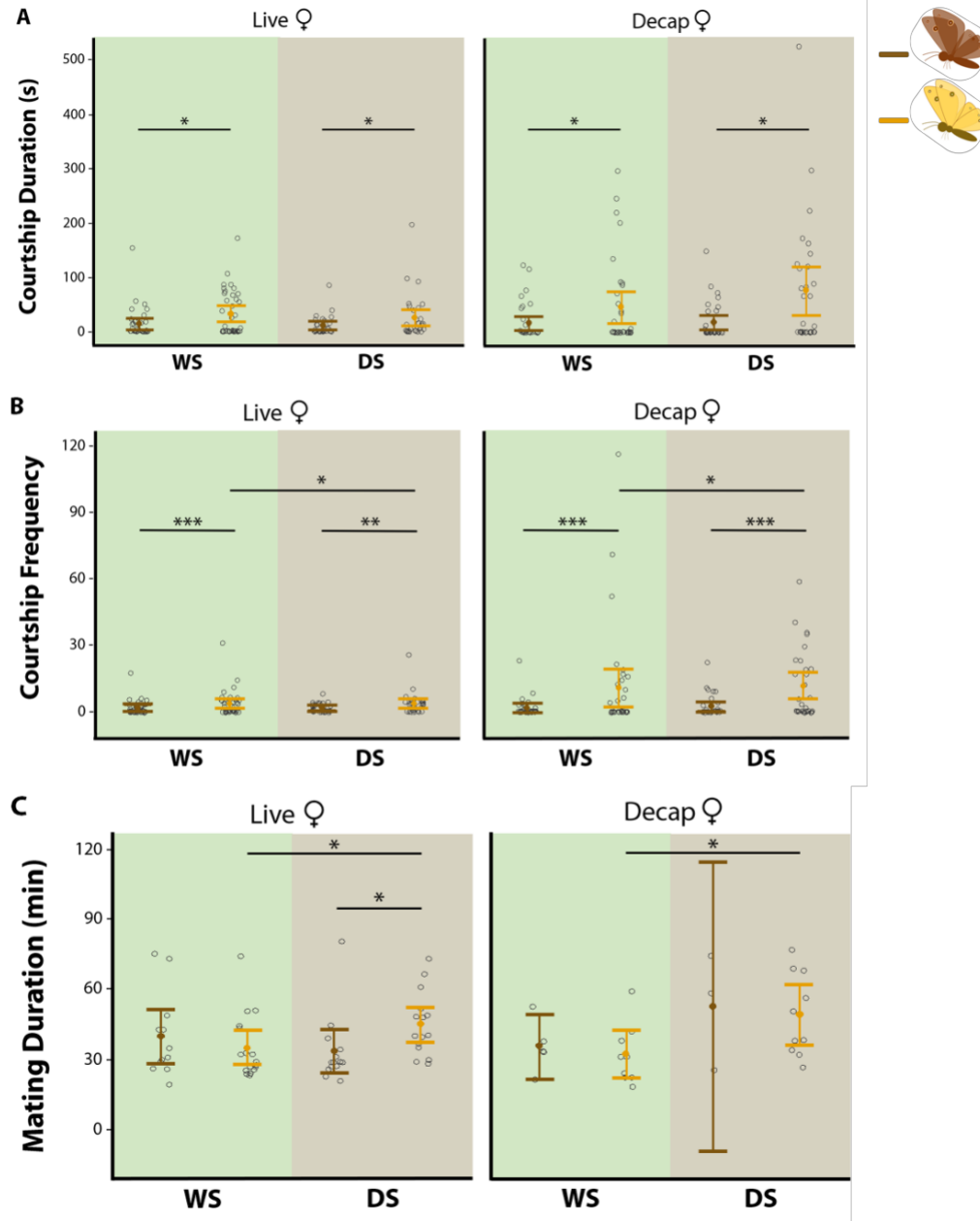
598

599

600 **Fig. 3.** Four hours after injections, *yellow* is downregulated in brains of DS pupae injected with  
601 20E compared to pupae injected with vehicle. Bars show fold change expression relative to WS  
602 pupae injected with vehicle solution. Indicated p values are the Turkey-adjusted p values from  
603 the post-hoc analysis.

604



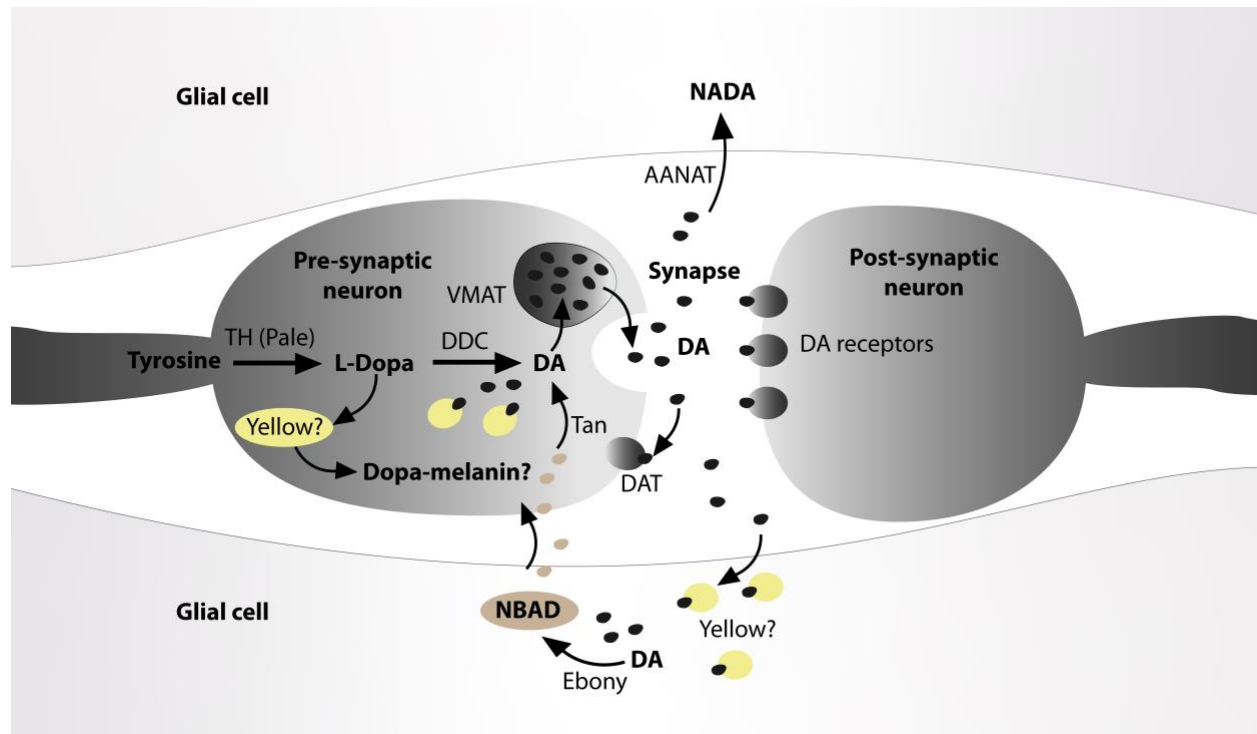


605  
606

607 **Fig. 4.** Courtship behavior of Wt and Yellow males, for wet (WS) and dry (DS) seasonal forms, in  
608 both live and decapitation assays. Yellow males courted at a higher duration and frequency than  
609 Wt males, for both WS and DS forms. DS Yellow males courted at a higher frequency and  
610 remained in copula for a longer period of time than WS Yellow males. **(A)** Courtship duration, **(B)**  
611 Courtship frequency and **(C)** Mating duration were quantified. Mating duration was quantified  
612 among mated males only. Vertical bars represent 95% confidence intervals. Open circles (°) are  
613 data points. Asterisks (\*) indicate significant differences: \* p ≤ 0.05, \*\* p ≤ 0.01, \*\*\* p ≤ 0.001.  
614 Outliers are not removed as they are true measurements. n(WS-Live-Wt) and n(WS-Live-Yellow)  
615 = 38, n(WS-Decap-Wt) and n(WS-Decap-Yellow) = 34, n(DS-Live-Wt), n(DS-Live-Yellow),  
616 n(DS-Decap-Wt) and n(DS-Decap-Yellow) = 30.

617

618



619

620

621 **Fig. 5.** Schematic model of a melanized dopaminergic neuron adapted from Yamamoto and Seto  
622 (36). In this model tyrosine is converted to L-Dopa which is converted to dopamine (DA) by  
623 Dopa decarboxylase (DDC). We hypothesize that *yellow* may also be expressed in dopaminergic  
624 neurons to convert L-Dopa to Dopa-melanin. Upregulation of *yellow* in DS pupal brains could  
625 decrease availability of L-Dopa to produce dopamine which is packaged into vesicles (VMAT)  
626 for release into the synapse. Another possibility is that *Yellow* binds to dopamine, reducing its  
627 availability either for direct synthesis of dopamine by DDC or indirectly (if it is also expressed in  
628 glial cells) by limiting the availability of dopamine conversion to NBAD by *Ebony*, which is  
629 converted back to dopamine by *Tan*. An excess of DA is converted to NADA by *AANAT* or is  
630 taken up by *DAT* back into the pre-synaptic neuron.

631

632 **References**

- 633 1. J. K. Neal, J. Wade, Courtship and copulation in the adult male green anole: effects of  
634 season, hormone and female contact on reproductive behavior and morphology. *Behav*  
635 *Brain Res* **177**, 177-185 (2007).
- 636 2. J. Meitzenn, C. K. Thompson, Seasonal-like growth and regression of the avian song  
637 control system- neural and behavioral plasticity in adult male Gambel's white-crowned  
638 sparrows. *Gen Comp Endocrinol.* **157**, 259-265 (2008).
- 639 3. P. M. Forlano, J. A. Sisneros, K. N. Rohmann, A. H. Bass, Neuroendocrine control of  
640 seasonal plasticity in the auditory and vocal systems of fish. *Front Neuroendocrinol* **37**,  
641 129-145 (2015).
- 642 4. A. D. Tramontin, E. A. Brenowitz, Seasonal plasticity in the adult brain. *Trends in*  
643 *Neurosciences* **23**, 251-258 (2000).
- 644 5. S. X. Zhang, E. H. Glantz, D. Rogulja, M. A. Crickmore, Hormonal control of  
645 motivational circuitry orchestrates the transition to sexuality in *Drosophila*. *bioRxiv*  
646 10.1101/852335 (2019).
- 647 6. A. Bear, A. Monteiro, Both cell-autonomous mechanisms and hormones contribute to  
648 sexual development in vertebrates and insects. *Bioessays* **35**, 725-732 (2013).
- 649 7. M. M. Elekonich, G. E. Robinson, Organizational and activational effects of hormones on  
650 insect behavior. *Journal of Insect Physiology* **46**, 1509-1515 (2000).
- 651 8. K. Wallen, The Organizational Hypothesis: Reflections on the 50th anniversary of the  
652 publication of Phoenix, Goy, Gerall, and Young (1959). *Horm Behav* **55**, 561-565 (2009).
- 653 9. K. Kimura, T. Hachiya, M. Koganezawa, T. Tazawa, D. Yamamoto, Fruitless and  
654 doublesex coordinate to generate male-specific neurons that can initiate courtship.  
655 *Neuron* **59**, 759-769 (2008).
- 656 10. A. Pandey, G. Bloch, Juvenile hormone and ecdysteroids as major regulators of brain and  
657 behavior in bees. *Current Opinion in Insect Science* **12**, 26-37 (2015).
- 658 11. H. H. Lin *et al.*, Hormonal Modulation of Pheromone Detection Enhances Male  
659 Courtship Success. *Neuron* **90**, 1272-1285 (2016).
- 660 12. L. Duportets, A. Maria, S. Vitecek, C. Gadenne, S. Debernard, Steroid hormone signaling  
661 is involved in the age-dependent behavioral response to sex pheromone in the adult male  
662 moth *Agrotis ipsilon*. *Gen Comp Endocrinol* **186**, 58-66 (2013).
- 663 13. J. W. Truman, L. M. Riddiford, Hormonal Mechanisms Underlying Insect Behaviour.  
664 *Advances in Insect Physiology* **10**, 297-352 (1974).
- 665 14. K. J. Argue, A. J. Yun, W. S. Neckameyer, Early manipulation of juvenile hormone has  
666 sexually dimorphic effects on mature adult behavior in *Drosophila melanogaster*. *Horm*  
667 *Behav* **64**, 589-597 (2013).
- 668 15. A. Bear, A. Monteiro, Male courtship rate plasticity in the butterfly *Bicyclus anynana* is  
669 controlled by temperature experienced during the pupal and adult stages. *PLoS One* **8**,  
670 e64061 (2013).
- 671 16. K. L. Prudic, C. Jeon, H. Cao, A. Monteiro, Developmental plasticity in sexual roles of  
672 butterfly species drives mutual sexual ornamentation. *Science* **331**, 73-75 (2011).
- 673 17. A. Bear, K. L. Prudic, A. Monteiro, Steroid hormone signaling during development has a  
674 latent effect on adult male sexual behavior in the butterfly *Bicyclus anynana*. *PLoS One*  
675 **12**, e0174403 (2017).

- 676 18. M. D. Drapeau, A. Radovic, P. J. Wittkopp, A. D. Long, A gene necessary for normal  
677 male courtship, yellow, acts downstream of fruitless in the *Drosophila melanogaster*  
678 larval brain. *J Neurobiol* **55**, 53-72 (2003).
- 679 19. J. H. Massey, D. Chung, I. Siwanowicz, D. L. Stern, P. J. Wittkopp, The yellow gene  
680 influences *Drosophila* male mating success through sex comb melanization. *Elife* **8**  
681 (2019).
- 682 20. E. Dion, A. Monteiro, J. Y. Yew, Phenotypic plasticity in sex pheromone production in  
683 *Bicyclus anynana* butterflies. *Sci Rep* **6**, 39002 (2016).
- 684 21. W. Li, A. Godzik, Cd-hit: a fast program for clustering and comparing large sets of  
685 protein or nucleotide sequences. *Bioinformatics* **22**, 1658-1659 (2006).
- 686 22. M. C. Neville *et al.*, Male-specific fruitless isoforms target neurodevelopmental genes to  
687 specify a sexually dimorphic nervous system. *Curr Biol* **24**, 229-241 (2014).
- 688 23. J. H. Massey, D. Chung, I. Siwanowicz, D. L. Stern, P. J. Wittkopp, The yellow gene  
689 influences *Drosophila* male mating success through sex comb melanization. *eLife* **8**,  
690 e49388 (2019).
- 691 24. K. A. Robertson, A. Monteiro, Female *Bicyclus anynana* butterflies choose males on the  
692 basis of their dorsal UV-reflective eyespot pupils. *Proc. R. Soc. B* **272**, 1541-1546  
693 (2005).
- 694 25. M. Huq, S. Bhardwaj, A. Monteiro, Male *Bicyclus anynana* Butterflies Choose Females  
695 on the Basis of Their Ventral UV-Reflective Eyespot Centers. *Journal of insect science*  
696 *(Online)* **19**, 25 (2019).
- 697 26. H. T. Spieth, *Drosophilid* mating behaviour- The behaviour of decapitated females.  
698 *Animal Behaviour* **14**, 226-235 (1966).
- 699 27. J. M. Ringo, "Hormonal Regulation of Sexual Behavior in Insects" in *Hormones, Brain*  
700 *and Behavior*. (2002), pp. 93-114.
- 701 28. R. H. Barth, L. J. Lester, Neuro-hormonal control of sexual behavior in insects. *Ann. Rev.*  
702 *Entomol.* **18**, 445-472 (1973).
- 703 29. H. Ishimoto, T. Sakai, T. Kitamoto, Ecdysone signaling regulates the formation of long-  
704 term courtship memory in adult *Drosophila melanogaster*. *Proc Natl Acad Sci U S A* **106**,  
705 6381-6386 (2009).
- 706 30. M. Bastock, A gene mutation which changes a behavior pattern. *Evolution* **10**, 421-439  
707 (1956).
- 708 31. M. D. Drapeau, S. A. Cyran, M. M. Viering, P. K. Geyer, A. D. Long, A cis-regulatory  
709 sequence within the yellow locus of *Drosophila melanogaster* required for normal male  
710 mating success. *Genetics* **172**, 1009-1030 (2006).
- 711 32. R. Wilson, B. Burnet, L. Eastwood, K. Connolly, Behavioural pleiotropy of the yellow  
712 gene in *Drosophila melanogaster*. *Genet Res* **28**, 75-88 (1976).
- 713 33. H. Verlinden, Dopamine signalling in locusts and other insects. *Insect Biochem Mol Biol*  
714 **97**, 40-52 (2018).
- 715 34. E. Petruccioli, A. Lark, J. A. Mrkvicka, T. Kitamoto, Significance of DopEcR, a G-  
716 protein coupled dopamine/ecdyseroid receptor, in physiological and behavioral response  
717 to stressors. *J Neurogenet* **34**, 55-68 (2020).
- 718 35. S. X. Zhang, D. Rogulja, M. A. Crickmore, Dopaminergic Circuitry Underlying Mating  
719 Drive. *Neuron* **91**, 168-181 (2016).

- 720 36. S. Yamamoto, E. S. Seto, Dopamine Dynamics and Signaling in Drosophila- An  
721 Overview of Genes, Drugs and Behavioral Paradigms. *Pigment Cell and Melanoma*  
722 *Research* **63**, 107-119 (2014).
- 723 37. H. Berek, A. Veraksa, M. Sugumaran, Drosophila melanogaster has the enzymatic  
724 machinery to make the melanic component of neuromelanin. *Pigment Cell Melanoma*  
725 *Res* **31**, 683-692 (2018).
- 726 38. P. J. Wittkopp, J. R. True, S. B. Carroll, Reciprocal functions of the Drosophila yellow  
727 and ebony proteins in the development and evolution of pigment patterns. *Developmental*  
728 *neurobiology* **129**, 1849-1858 (2002).
- 729 39. J. Li, B. M. Christensen, *Biological Function of Insect Yellow Gene Family*. T. Liu,  
730 LeKang, Eds., Recent Advances in Entomological Research From Molecular Biology to  
731 Pest Management. (Springer, 2011).
- 732 40. X. Xu *et al.*, Structure and function of a "yellow" protein from saliva of the sand fly  
733 Lutzomyia longipalpis that confers protective immunity against Leishmania major  
734 infection. *J Biol Chem* **286**, 32383-32393 (2011).
- 735 41. I. Y. Rauschenbach *et al.*, Mechanisms of age-specific regulation of dopamine  
736 metabolism by juvenile hormone and 20-hydroxyecdysone in Drosophila females. *J*  
737 *Comp Physiol B* **181**, 19-26 (2011).
- 738 42. B. Zilberman-Peled, B. Ron, A. Gross, J. P. Finberg, Y. Gothilf, A possible new role for  
739 fish retinal serotonin-N-acetyltransferase-1 (AANAT1): Dopamine metabolism. *Brain*  
740 *Res* **1073-1074**, 220-228 (2006).
- 741 43. I. Y. Rauschenbach *et al.*, Dopamine effect on 20-hydroxyecdysone level is mediated by  
742 juvenile hormone in Drosophila females. *Dokl Biochem Biophys* **446**, 263-265 (2012).
- 743 44. L. L. Ellis, G. E. Carney, Mating alters gene expression patterns in Drosophila  
744 melanogaster male heads. *BMC Genomics* **11**, 558 (2010).
- 745 45. N. E. Gruntenko *et al.*, An increase in the dopamine level accelerates sexual maturation  
746 of Drosophila melanogaster deficient in the juvenile hormone. *Dokl Biol Sci* **406**, 88-90  
747 (2006).
- 748 46. K. Harano, K. Sasaki, T. Nagao, M. Sasaki, Influence of age and juvenile hormone on  
749 brain dopamine level in male honeybee (*Apis mellifera*): association with reproductive  
750 maturation. *J Insect Physiol* **54**, 848-853 (2008).
- 751 47. N. E. Gruntenko, E. K. Karpova, N. A. Chentsova, N. V. Adonyeva, I. Y. Rauschenbach,  
752 20-hydroxyecdysone and juvenile hormone influence tyrosine hydroxylase activity in  
753 Drosophila females under normal and heat stress conditions. *Arch Insect Biochem Physiol*  
754 **72**, 263-272 (2009).
- 755 48. F. D. Karim, G. M. Guild, C. S. Thummel, The Drosophila Broad-Complex plays a key  
756 role in controlling ecdysone-regulated gene expression at the onset of metamorphosis. .  
757 *Development* **118**, 977-988 (1993).
- 758 49. Z. Gauhar *et al.*, Genomic mapping of binding regions for the Ecdysone receptor protein  
759 complex. *Genome Res* **19**, 1006-1013 (2009).
- 760 50. A. M. Bolger, M. Lohse, B. Usadel, Trimmomatic: a flexible trimmer for Illumina  
761 sequence data. *Bioinformatics* **30**, 2114-2120 (2014).
- 762 51. M. G. Grabherr *et al.*, Full-length transcriptome assembly from RNA-Seq data without a  
763 reference genome. *Nat. Biotechnol.* **29**, 644-652 (2011).
- 764 52. B. J. Haas *et al.*, De novo transcript sequence reconstruction from RNA-seq using the  
765 Trinity platform for reference generation and analysis. *Nat Protoc* **8**, 1494-1512 (2013).

- 766 53. B. Li, C. N. Dewey, RSEM: accurate transcript quantification from RNA-Seq data with  
767 or without a reference genome. *BMC Bioinformatics* **12**, 323 (2011).
- 768 54. B. Langmead, C. Trapnell, M. Pop, S. L. Salzberg, Ultrafast and memory-efficient  
769 alignment of short DNA sequences to the human genome. *Genome Biology* **10**, R25  
770 (2009).
- 771 55. M. Robinson, D. McCarthy, G. Smyth, edgeR: a Bioconductor package for differential  
772 expression analysis of digital gene expression data. *Bioinformatics* **26**, 139-140 (2010).
- 773 56. R. W. Nowell *et al.*, A high-coverage draft genome of the mycalesine butterfly *Bicyclus*  
774 *anyana*. *GigaScience* **6**, 1-7 (2017).
- 775 57. Q. Zhang *et al.*, TqPCR: A Touchdown qPCR Assay with Significantly Improved  
776 Detection Sensitivity and Amplification Efficiency of SYBR Green qPCR. *PLOS ONE*  
777 **10**, e0132666 (2015).
- 778 58. M. T. Ganger, G. D. Dietz, S. J. Ewing, A common base method for analysis of qPCR  
779 data and the application of simple blocking in qPCR experiments. *BMC Bioinformatics*  
780 **18**, 534 (2017).
- 781 59. R Development Core Team (2020) R: A language and environment for statistical  
782 computing. ed R. F. f. S. Computing (ISBN 3-900051-07-0, Vienna, Austria).
- 783 60. RStudio Team (2020) RStudio: Integrated Development for R. <http://www.rstudio.com/>.  
784 ed R. Inc. (Boston, MA).
- 785 61. R. M. Hope (2013) Rmisc: Ryan Miscellaneous. R package version 1.5. .
- 786 62. J. Fox, S. Weisberg, *An {R} Companion to Applied Regression, Third Edition*. T. O. C.  
787 Sage, Ed. (2019).
- 788 63. R. V. Lenth, emmeans: Estimated Marginal Means, aka Least-Squares Means. R package  
789 version 1.4.6., 1 (2020).
- 790 64. H. Miura, R. M. Quadros, C. B. Gurumurthy, M. Ohtsuka, Easi-CRISPR for creating  
791 knock-in and conditional knockout mouse models using long ssDNA donors. *Nat Protoc*  
792 **13**, 195-215 (2018).
- 793 65. F. Mery *et al.*, Public versus personal information for mate copying in an invertebrate.  
794 *Curr. Biol.* **19**, 730-734 (2009).
- 795 66. C. M. Nieberding *et al.*, The male sex pheromone of the butterfly *Bicyclus anyana*:  
796 towards an evolutionary analysis *Plos ONE* **3**, e2751 (2008).
- 797 67. P. K. Dunn, Tweedie: Evaluation of Tweedie exponential family models. R package  
798 version 2.3. (2017).
- 799 68. S. Jackman, pscl: Classes and Methods for R Developed in the Political Science  
800 Computational Laboratory, R package version 1.5.5. *United States Studies Centre,*  
801 *University of Sydney, Sydney, New South Wales, Australia.* (2020).
- 802 69. R. Maia, C. M. Eliason, P.-P. Bitton, S. M. Doucet, M. D. Shawkey, pavo: an R Package  
803 for the analysis, visualization and organization of spectral data. *Methods in Ecology and*  
804 *Evolution* **4**, 609-613 (2013).
- 805

## Supplementary data and information

### Supplementary tables

**Table S1.** Assembly statistics for *B. anynana* brain transcriptome

Type	Assembly statistics
Total Trinity genes	689,657
Total Trinity transcripts	1,403,420
Percent GC	36.50
Median contig length (bp)	456
Average contig length (bp)	703.17
N50 (bp)	973
Total assembled bases	986,848,704

**Table S2 (excel file).** Differentially expressed genes of male pupal brains comparisons between treatments (Dry season with vehicle - DSV, Wet season with vehicle - WSV and Dry season injected with 20E - DS20E. logFC represents the log-foldchange in the gene expression; logCPM represents the log counts per million; FDR represents the false discovery rate, where values of less than 0.001 are simply represented as <0.001. **See excel file** sheet 1 for DSV compared to WSV, sheet 2 for DS20E compared to DSV, and sheet 3 for DS20E compared to WSV. Green color indicates down-regulated genes and red indicates upregulated genes.



**Table S3.** Differentially expressed genes associated with neural development.

<b>Genes</b>	<b>Function</b>	<b>References</b>
<i>asteroid</i>	Involved in the epidermal growth factor receptor signaling pathway in <i>Drosophila</i> and could affect the differentiation of photoreceptor cells in eye development. Asteroid is also crucial for the specification of muscle tissues.	Higson, Tessiatore et al. (1993), Kotarski, Leonard et al. (1998), Ruden, Wang et al. (1999), Artero, Furlong et al. (2003)
<i>Integrin beta pat-3, βPS</i>	Integrins are a large family of transmembrane molecules that mediate cell and extracellular matrix interactions, ubiquitous in multicellular animals. In <i>Drosophila</i> , integrins are essential for normal gonad development. <i>βPS</i> plays a role in eye development at the late pupal stage for photoreceptor cell organization.	Reviewed by Johnson, Lu et al. (2009), Chen, Lewallen et al. (2013). Tanentzapf, Devenport et al. (2007), O'Reilly, Lee et al. (2008) Zusman, Patel-King et al. (1990), Zusman, Grinblat et al. (1993)
<i>Lactoylglutathione lyase, Glo1</i>	Part of the glyoxalase system present in the cytosol of all cells and catalyzes the detoxification of methylglyoxal, a by-product of metabolism. Methylglyoxal (MG) inhibits cell division in a range of organisms by interfering with protein, DNA and RNA synthesis and can lead to the damage of cells through the production of precursors that react with intracellular and extracellular proteins. The effect of Glo1 expression on behavior was studied in male mice, where higher expression of Glo1 was associated with less locomotor activity in mice with Glo1 knockout mice moving and exploring significantly more than wildtype mice.	Reviewed by Thornalley (2003) Együd and Szent-Györgyi (1966), Együd and Szent-Györgyi (1966), Krymkiewicz, Diéguez et al. (1971), Brownlee (2001) Williams, Lim et al. (2009), Jang, Kwon et al. (2017)
<i>lethal 2 essential for life, l(2)efl</i>	Involved in neurite extension and synapse morphology, <i>l(2)efl</i> expression is upregulated in the brains of older bees, a finding that has been replicated in other studies comparing foragers and nurse bees <i>l(2)efl</i> may be required for behavioral maturation of adult workers and also neural plasticity as it was upregulated in honeybees exposed to light.	Becker, Kucharski et al. (2016) Kucharski and Maleszka (2002), Garcia, Saraiva Garcia et al. (2009).
<i>neural Wiskott-Aldrich syndrome protein (N-WASP)</i>	Involved in the organization of actin cytoskeleton and neurite outgrowth.	Suetsugu, Hattori et al. (2002)
<i>neuropeptide CCHamide2</i>	Produced in both the midgut and the brain. CRISPR mutants of <i>CCHamide2</i> show reductions in feeding, delayed larval development, smaller wings and reduced adult locomotor activity during foraging hours	Ren, Hauser et al. (2015)
<i>osiris genes</i>	Essential housekeeping functions. Osiris genes have been associated with pathogen response, developmental stage and the degree of melanisation.	Dorer, Rudnick et al. (2003), Shah, Dorer et al. (2012), Cornman, Lopez et al. (2013), McTaggart, Hannah et al. (2015), Wu, Tong et al. (2016), Yang, Huang et al. (2016), Andrade López, Lanno et al. (2017)
<i>SKI family transcriptional corepressor 2</i>	SKOR2 is expressed in human and murine neuronal tissues in embryogenesis and also adult tissues	(Arndt, Poser et al. 2005, Mizuhara, Nakatani et al. 2005, Minaki, Nakatani et al. 2008, Wang, Harrison et al. 2011, Nakatani, Minaki et al. 2014)

**Table S4.** Primers used in the qPCR experiment

Gene	Primers
Elongation Factor-1 $\alpha$ (EF-1 $\alpha$ )	Forward: 5'- GTGGGCGTCAACAAAATGGA-3' Reverse: 3'- GCAAAAACAACGAT-5'
<i>yellow</i>	Forward: 5'- TATACCTCTGGATGCGCCCT-3' Reverse: 3'- AGAGTAAGGACAAACATTCGTCACA-5'

## Supplementary Figures

**Fig. S1.** Summary of N50 contig lengths against ExN50 values

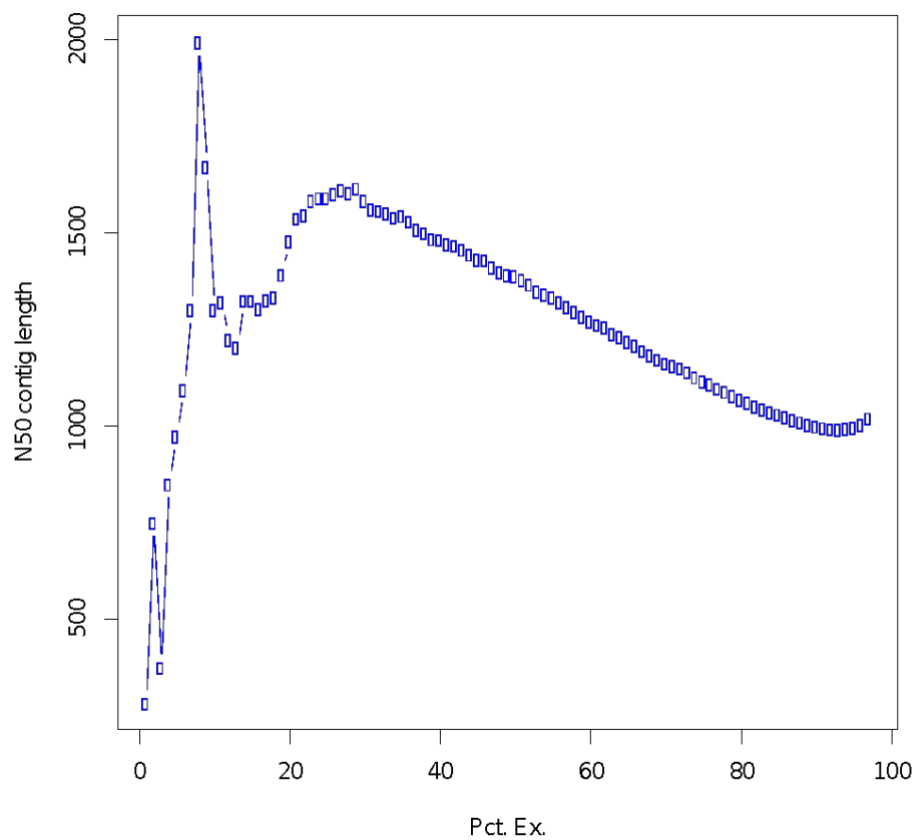


**Fig. S2.** Clustering analysis of transcripts across 12 libraries. Colored bars at the base of the dendrogram indicate libraries of the three treatments – blue bar: wet season (S1, S12, S17); red bar: dry season with 20E (S2, S3, S6, S8, S15) and green bar: dry season (S4, S5, S7, S9). Dendrogram on the left represents the clustering of transcript expression based on the frequency of their expression together. The color of transcripts indicates their relative expression. The color key indicates the range of colors representing the fold change difference in expression.

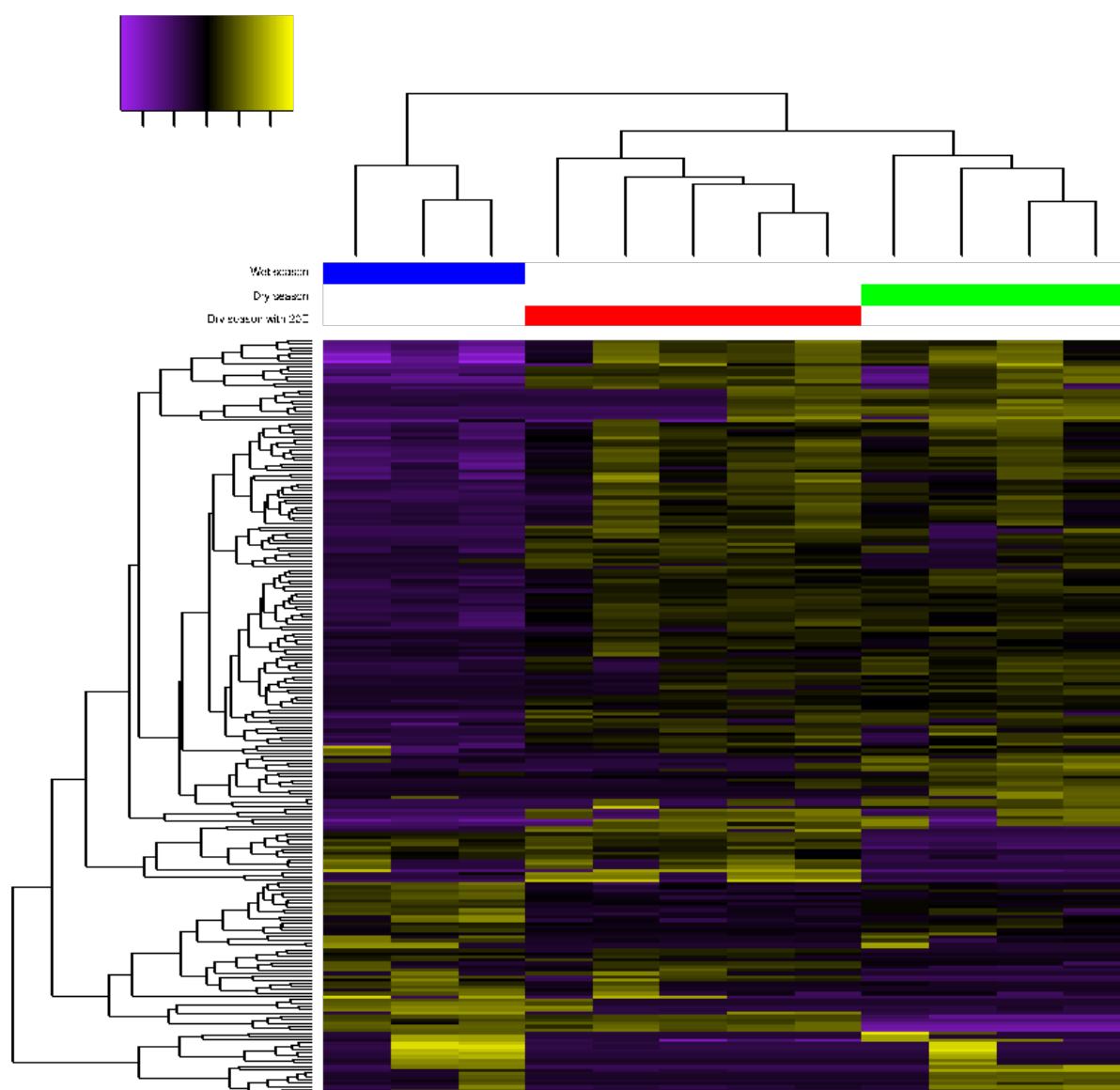


**Fig. S3.** Expression level of yellow in brains of vehicle- and 20E-injected DS pupae dissected 2 hours, 4 hours and 24 hours after injections. Levels of expression are calculated relative to the baseline groups, all WS pupae injected with vehicle solution (at the value of 1, from 5 biological replicates at 2h and 4 replicates at 4 and 24 h) and dissected at the same time as DS individuals (5 biological replicates in all DS groups). Indicated p are the Tukey adjusted p values from the post-hoc analysis).

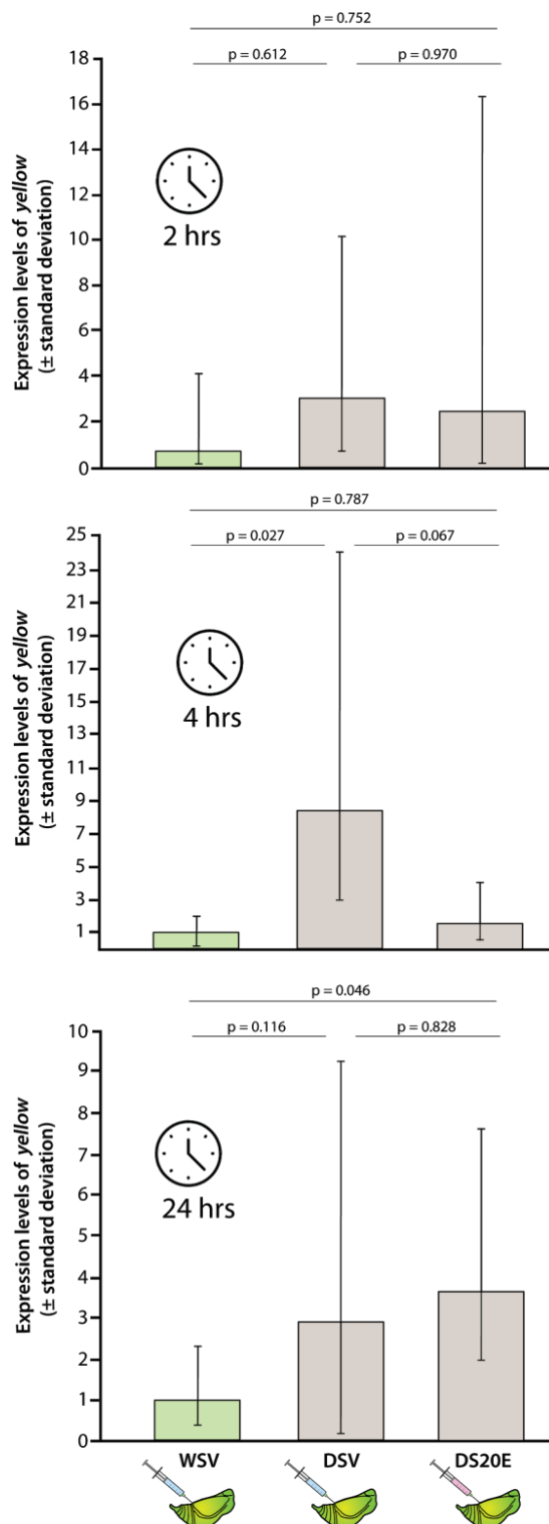
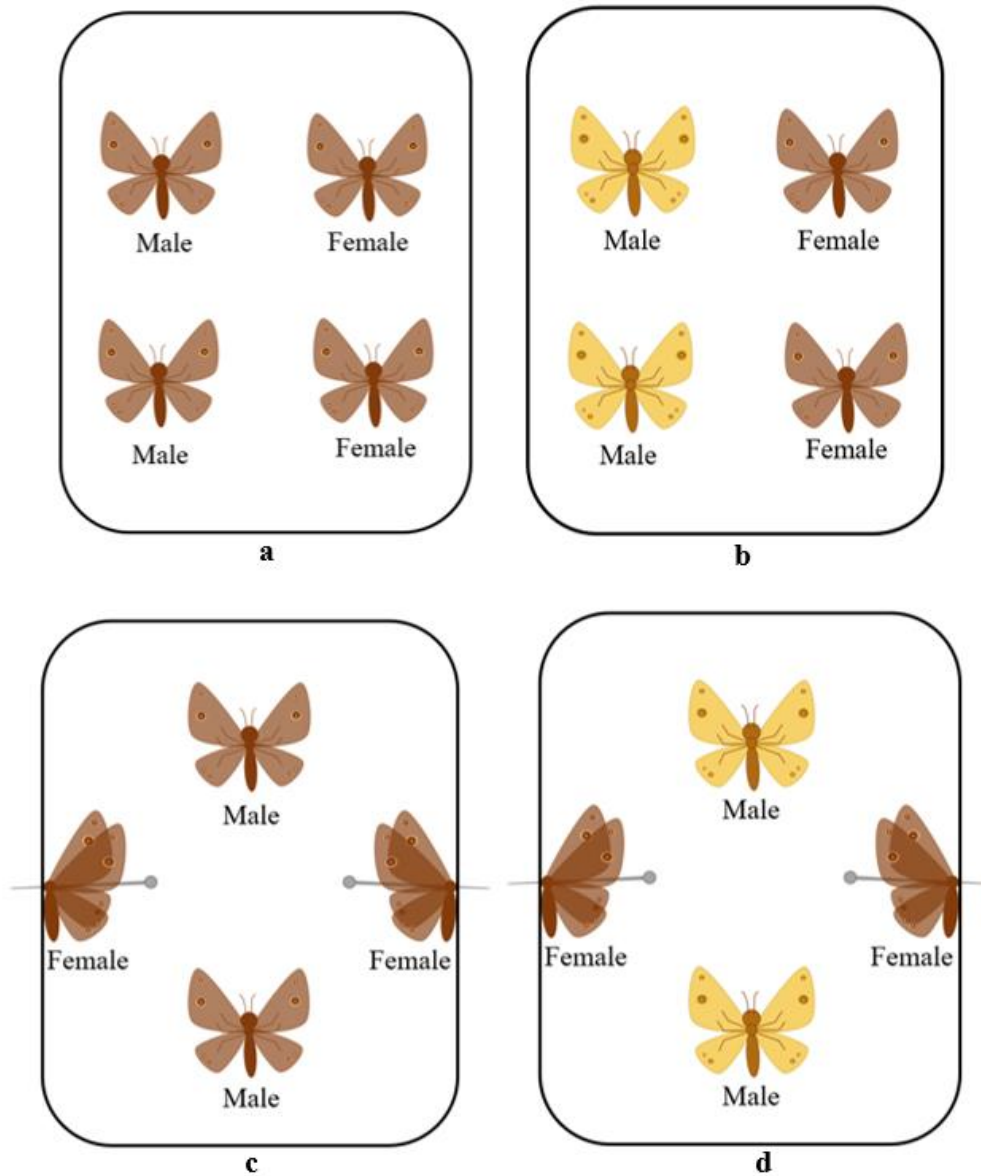


**Fig. S4.** Experimental design of the live (**a-b**) and decapitation (**c-d**) experiments. Two males and two females (live or decapitated) were put in one cage and left under UV light for one hour of observation. Quantification of courtship begins once the UV light is switched on, until the mating of individual butterflies. **(a)** Two Wt males and two Wt females; **(b)** two Yellow males and two Wt females; **(c)** two Wt males and two decapitated Wt females; **(d)** two Yellow males and two decapitated Wt females. These were done on wet season (WS) and dry season (DS) butterflies.



## **Supplementary Methods for Fig. S5 (next page)**

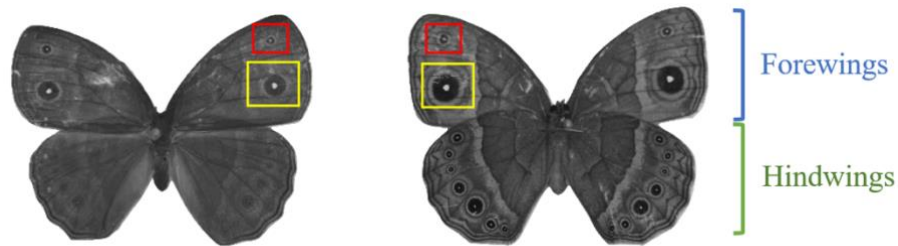
### *UV photography and spectrophotometry*

To measure the UV reflectivity of the Yellow mutant and Wt male forewing eyespots on both the ventral and dorsal sides (Fig. S5), WS butterflies were photographed using a Nikon D7100 digital camera with a Jenoptik CoastalOpt 105 mm UV – Vis crystal lens under sunlight. Visible light was captured through a Baader UV/IR Cut Filter (transmits 400 to 680 nm) and UV images were taken through a Baader U-Venus Filter (transmits 320 to 380 nm). The camera settings were ISO100 and a shutter speed of 1/320 seconds for visible light and 10 seconds for UV light.

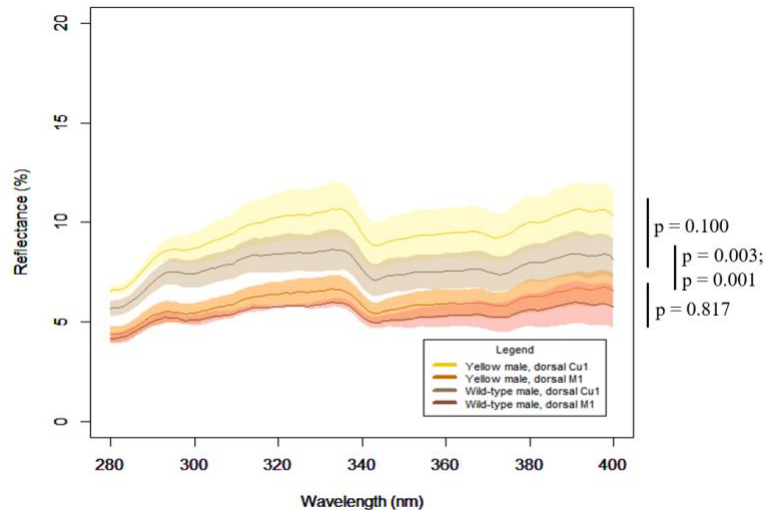
Scale reflectance was measured at the two forewing eyespots using a gonio-spectrophotometer and the accompanying program, OceanView 1.6.7 (Ocean Optics). Each measurement was taken with the axis of the illuminating and detecting fibre directed at a 20° angle to the plane of the wing at a using a deuterium-halogen tungsten lamp (DH-2000, Ocean Optics) as a standardized light source and calibrated using a white Ocean Optics WS-1 reflectance standard. from the right forewing. A total of three replicates were done for each type and sex.

**Fig. S5.** WS Yellow mutant and Wt males have similar UV reflectivity of both forewing eyespots on both sides of the wing. **(A)** shows both the dorsal (left) and ventral (right) sides of a Wt butterfly, M1 and Cu1 eyespots are indicated by red and yellow squares respectively. Graphs show the mean smoothed reflectance spectra ( $\pm$ standard deviation,  $n=3$ ) of WS Yellow mutant and Wt butterflies (280 – 400 nm). The legend for each graph is shown on the bottom right: yellow – Yellow mutant Cu1, orange – Yellow mutant M1, brown – Wt Cu1, red – Wt M1. **(B)** Male Yellow and Wt *B. anynana*, dorsal Cu1 and M1; **(C)** Male Yellow and Wt *B. anynana*, ventral Cu1 and M1.

**A**



**B**



**C**

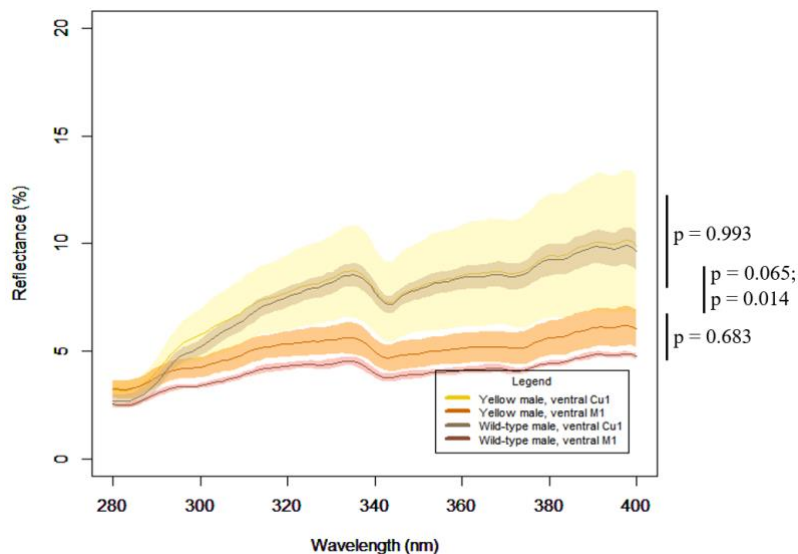




**Fig. S6.** Courtship behavior of Wt and Yellow males, for wet (WS) and dry (DS) seasonal forms, in both live and decapitation assays. **(A)** Latency to mate and **(B)** Percentage of matings were quantified among mated males only. Vertical bars represent 95% confidence intervals. Open circles (°) are data points. Asterisks (\*) indicate significant differences: \*  $p \leq 0.05$ , \*\*  $p \leq 0.01$ , \*\*\*  $p \leq 0.001$ . Outliers are not removed as they are true measurements.  $n(\text{WS-Live-Wt})$  and  $n(\text{WS-Live-Yellow}) = 38$ ,  $n(\text{WS-Decap-Wt})$  and  $n(\text{WS-Decap-Yellow}) = 34$ ,  $n(\text{DS-Live-Wt})$ ,  $n(\text{DS-Live-Yellow})$ ,  $n(\text{DS-Decap-Wt})$  and  $n(\text{DS-Decap-Yellow}) = 30$ .

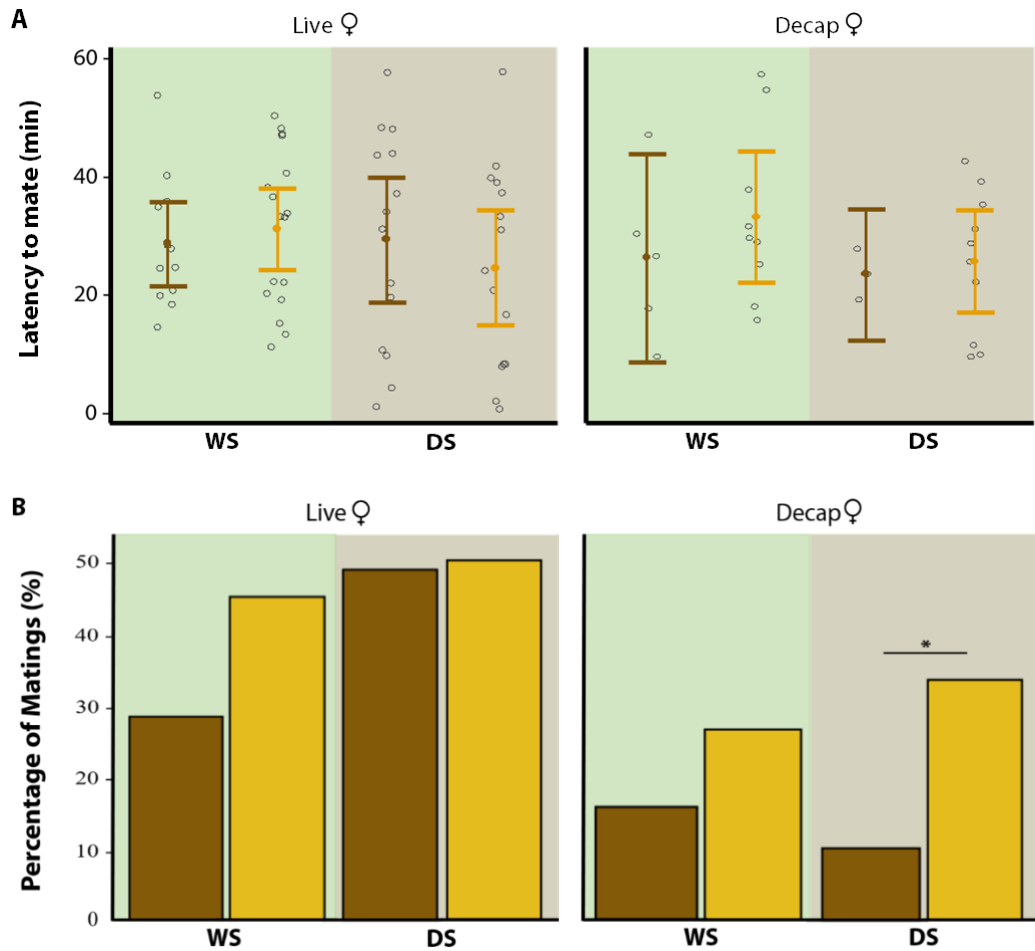


**Fig S7.** Generation of the Yellow-attP mutant knockout line. **(A)** Insertion of an attP sequence into exon 4 (annotated using LepBase ensemble), the attP insertion is shown in red, the major royal jelly domain is shown in green. **(B)** Gel images of the haemolymph PCR for identifying transgenic individuals. Gel **a** shows the PCR products using primers designed to the attP insert. Gel **b** shows the PCR products using primers designed to the *yellow* coding sequence spanning the attP insertion which reveals which animals are heterozygous or homozygous based on the number and size of the PCR band. Individual no. 1 shows 2 bands thus has both the Wt and attP genome. Individual no. 2 shows only 1 band which is slightly larger meaning it has the attP genome only. Individual no. 5 shows only a single small band thus has the Wt genome only. **(C)** Alignment of the yellow sequence with the corresponding region from the yellow-attP line. **(D)** Phenotype of the Yellow mutant knockout butterflies (left) and Wt (right).

